

Review of International Geographical Education | RIGEO | 2020

# RIGEO

ISSN: 2146 - 0353

## Review of International GEOGRAPHICAL EDUCATION



[www.rigeo.org](http://www.rigeo.org)

# SEAIR Model for COVID-19 Transmission Dynamics in Chennai, Tamil Nadu: Analysis and Parameter Estimation Through Optimization Algorithms

Jeshua Rajan<sup>1,2\*</sup>, G. Jeyakumar<sup>3</sup>

<sup>1</sup>Research Scholar (Reg.No.18121272091030), St. John's College, Palayamkottai, Affiliated to Manonmaniam Sundaranar University, Abishekapatti, Tirunelveli 627 012, Tamil Nadu, India

<sup>2</sup>Lecturer / Mathematics, Department of Basic Engineering, Government Polytechnic college, R.K. Nagar, Chennai 600 081, Tamil Nadu, India

<sup>3</sup>Associate Professor and Head (Rtd.), Department of Mathematics, St. John's College, Palayamkottai, Tirunelveli 627 002, Tamilnadu, India

\*Corresponding author email: [jeshuarajan@gmail.com](mailto:jeshuarajan@gmail.com);

## Abstract

**Objectives:** This study sets up an ordinary differential model, SEAIR, analyzing the transmission dynamics of COVID-19, where human population is divided into five compartments: Susceptible ( $S$ ), Exposed ( $E$ ), Asymptomatic Infected ( $A$ ), Symptomatic Infected ( $I$ ), and Recovered ( $R$ ). The final purpose would be to have a framework that helps in analysis of stability and conditions regarding the pandemic for both the disease-free and endemic states. **Methods:** This SEAIR model is solved through equilibrium analysis in order to distinguish between the two equilibria-disease-free and endemic-states of the disease. Equilibrium conditions for the stability conditions are found using the  $\mathcal{R}_0$  number calculated by means of the next-generation matrix method to understand the likelihood of disease persistence. The dataset has been taken from the daily reports on the active COVID-19 cases in Chennai, reported by the Government of Tamil Nadu. Numerical simulations of the SEAIR model is conducted by using the *odeint* function from the *scipy.integrate* library in Python. Model validation was achieved by fitting the SEAIR model to real COVID-19 data from Chennai, Tamil Nadu using optimization algorithms including Nelder-Mead, Differential Evolution, Genetic Algorithm, L-BFGS-B, Particle Swarm Optimization, and Powell's algorithm for parameter estimation. **Findings:** The model shows that when the number of new infectious cases from both asymptomatic and symptomatic individuals is below unity, the disease-free equilibrium is locally asymptotically stable. The model reaches and maintains an endemic equilibrium if the basic reproduction number is greater than unity. This model was fit to the observed data using several optimization algorithms used and thus showing a clear fit between the observed values and the modelled prediction. **Novelty:** This research presents an effective SEAIR model strong enough to explain COVID-19 transmission appropriately in urban settings and, therefore, represents an important resource to direct intervention in public health.

**Keywords:** Mathematical Modeling, Equilibrium Analysis, Basic Reproduction Number, Parameter Estimation, Optimization Algorithm.

## 1. Introduction

Compartmental models are the most useful in that they bring together very complex biological processes into mathematical frameworks which could be solved. Among those commonly used are the models SIR, Susceptible-Infectious-Recovered, and SEIR, Susceptible-Exposed-Infectious-Recovered. These models have had compartments added to them as better representations of the severity of certain diseases. One example is the SEAIR model: Susceptible-Exposed-Asymptomatic-Infected-Recovered, which became highly relevant in the context of COVID-19. The number of asymptomatic carriers was a major conduit of disease transmission.

Asymptomatic infection is an important feature that has been added to most researchers' versions of the SEIR model. Anastassopoulou *et al.* extended the SEIR model to an asymptomatic compartment, and they were able to demonstrate the role of asymptomatic carriers in the epidemic curve [1]. Giordano *et al.* developed an extended SEIR model including compartments for asymptomatic, diagnosed, and ailing individuals in order to capture the spread of COVID-19 in Italy better [2]. Another developed model includes asymptomatic infection besides public health interventions for enhanced consideration of the COVID-19 disease transmission dynamics [3]. A different version of an SEIR model considers vaccination along with a few public health measures so as to predict the time- evolution dynamics of this disease [4]. The impact of mobility restrictions and vaccination in heterogeneous populations has been studied, which has highlighted the need for accounting for diversity in the population in modeling efforts [5]. A network-based approach has been used to model the effects of contact tracing and testing on the spread of COVID-19 [6].

Environmental variables including temperature and humidity have been assessed through Bayesian spatiotemporal, thereby enhancing the COVID-19 model complexity. An analysis regarding vaccination and booster doses, focusing on ongoing immunization efforts has also been reported [7]. Studies regarding Wuhan, China, analyze how public health measures affect controlling the spread of the virus [8]. Research has focused more on vaccination strategies. In this regard, models have been developed to examine age-specific vaccination strategies and their potential impact on transmission dynamics [9]. Models of COVID-19 transmissions in high-density urban areas have also been developed with consideration for social contact patterns and implemented public health measures [10]. Implications of vaccine coverage and effectiveness in rural settings have been discussed in [11]. Various booster doses have been accounted for in terms of transmission dynamics and control measures [12]. Vaccine hesitancy and public health measures among diverse populations have also been taken into consideration, based on the challenges related to universal immunity levels. [13]

Parameter estimation is a major key to the accuracy of any epidemiological model. There are various optimization algorithms which have been used for efficient estimation of model parameters. The Nelder-Mead method, Differential Evolution, Genetic Algorithms, and other optimization techniques have been used for fitting models to real-world data. Wang *et al.* used L-BFGS-B algorithms to estimate parameters of the COVID-19 model from Wuhan, China; this fitted the data so well and provided reliable prediction results [14]. Rabajante used Particle Swarm Optimization to estimate the parameters for an SEAIR model with COVID-19; his study demonstrated the model as a good fit for dynamics in the disease [15].

The basic reproduction number ( $\mathcal{R}_0$ ) is a metric in epidemiological modeling representing the average number of secondary infections produced by an infectious individual in a fully susceptible population. There have been many studies on deriving  $\mathcal{R}_0$  for COVID-19 using different models. The next-generation matrix method was first proposed by Diekmann *et al.* as a standard approach for computing  $\mathcal{R}_0$  in compartmental models. [16] This approach has been widely applied to the COVID-19 models of determining the disease-free and endemic equilibria conditions. [17]

Asymptomatic carriers have a disproportionately large impact on the spread of COVID-19 since their infections are often asymptomatic. He *et al.* and Mizumoto *et al.* argued that asymptomatic transmission was a key component in the initial phases of the pandemic. [18], [19] Their research illustrates the inclusion of such asymptomatic compartment in any epidemiological model is vital for reflecting realities appropriately.

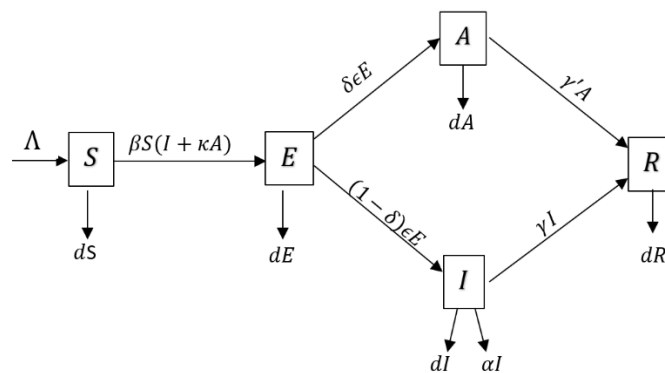
Modeling studies have highlighted the effective use of public health intervention measures such as social distancing, quarantine, and vaccines. Ferguson *et al.* applied an extended SEIR model to evaluate the impact of non-pharmaceutical measures on the spread of SARS-CoV-2 in the UK and in the US to inform policy for the pandemic period [20]. Similarly, Hellewell *et al.* and Prem *et al.* applied the compartmental models to discuss the effect of different interventional strategies on the COVID-19 transmission dynamics [21], [22]. Omede *et al.* have analyzed the Delta and Omicron variants of the virus within the United States [23]. Kim *et al.* have analyzed on the multi-variant model within an optimal control strategy for the control of the disease within Ghana [24]. Hu *et al.* assessed COVID-19 dynamics regarding stability within the United States [25], whereas Riaz *et al.* investigated a nonlinear model related to environmental and social influences on the pandemic in assessing pandemic control measures [26]. Zerefe *et al.* also studied contact tracing with regard to the transmission of COVID-19 in Ethiopia, demonstrating its effectiveness in controlling outbreaks [27].

The rest of the paper is structured as follows. In Section 2, we derive the SEAIR mathematical model and explain in detail each variable and parameter. In Section 3, we discuss the mathematical analysis of the model, including boundedness of the system, existence of equilibrium points, the basic reproduction number, and stability analysis of the equilibrium points. In Section 4, we apply COVID-19 data from Chennai, Tamil Nadu, collected between May 3, 2020, and August 7, 2022, to estimate the parameters such as the transmission rate, recovery rate, and the progression rate from exposed to infectious [28]. For the estimation, we applied six optimization algorithms: Nelder-Mead Algorithm, Differential Evolution Optimization, Genetic Algorithm, L-BFGS-B Algorithm, Particle Swarm Optimization, and Powell's Algorithm. We will then compare the estimated parameters and goodness-of-fit of each algorithm to gauge their accuracy. Finally, in Section 5, we will present our concluding remarks and some implications drawn from the paper.

## 2. Methodology

The mathematical model for COVID-19 transmission is a compartmental model that divides the total human population ( $N$ ) into five distinct compartments: Susceptible ( $S$ ), Exposed ( $E$ ), Symptomatic Infected ( $I$ ), Asymptomatic Infected ( $A$ ) and Recovered ( $R$ ) population as shown in the Figure 1. Each compartment represents a different stage in the progression of the disease within the population.

**Figure 1.** SEAIR Block Diagram: Dynamics of the model



Susceptible ( $S$ ) compartment includes individuals who have not yet been infected with COVID-19 but are at risk of infection upon contact with infected individuals. Exposed ( $E$ ) compartment consists of individuals who have been infected with COVID-19 but are not yet infectious belong to this compartment. This stage represents the incubation period. Symptomatic Infected ( $I$ ) compartment consists of individuals who are infected with COVID-19 and exhibit symptoms. These individuals are infectious and contribute to the transmission of the disease. Asymptomatic Infected ( $A$ ) includes individuals who are infected with COVID-19 but do not exhibit symptoms. Despite the lack of symptoms, they are still infectious, although potentially less so than symptomatic individuals. Recovered ( $R$ ) compartment includes individuals who have recovered from the infection and gained immunity belong to this compartment. They are no longer infectious.

The model is formulated as a system of nonlinear autonomous first-order differential equations that describe the rate of change of each compartment over time:

$$\left\{ \begin{array}{l} \frac{dS}{dt} = \Lambda - \beta S(I + \kappa A) - dS \\ \frac{dE}{dt} = \beta S(I + \kappa A) - (\epsilon + d)E \\ \frac{dA}{dt} = \delta \epsilon E - (\gamma' + d)A \\ \frac{dI}{dt} = (1 - \delta) \epsilon E - (\gamma + \alpha + d)I \\ \frac{dR}{dt} = \gamma I + \gamma' A - dR \end{array} \right. \quad (1)$$

The parameters of the model are defined as follows:  $\Lambda$  represents the recruitment rate of new susceptible individuals into the population,  $\beta$  is the transmission rate of the disease, and  $\kappa$  denotes the relative infectiousness of asymptomatic individuals compared to symptomatic individuals. The parameter  $d$  is the natural death rate of individuals, while  $\epsilon$  indicates the rate at which exposed individuals become infectious. The proportion of exposed individuals who become asymptomatic is denoted by  $\delta$ , and the recovery rates of symptomatic and asymptomatic infected individuals are represented by  $\gamma$  and  $\gamma'$ , respectively. And,  $\alpha$  is the disease-induced death rate of symptomatic infected individuals.

The model dynamics describe the changes in each compartment over time. The susceptible population ( $S$ ) decreases due to new infections and natural deaths but increases with the recruitment of new individuals. The exposed population ( $E$ ) increases as susceptible individuals come into contact with the virus and transition into the exposed state. This compartment decreases as exposed individuals either progress to the infectious stages or die. The asymptomatic infected population ( $A$ ) grows as a proportion ( $\delta$ ) of exposed individuals develop asymptomatic infections and decreases as these individuals either recover or die. On the other hand, the symptomatic infected population ( $I$ ) increases as a proportion ( $1 - \delta$ ) of exposed individuals develop symptoms. This compartment decreases due to recovery, disease-induced deaths, or natural deaths. The recovered population ( $R$ ) increases as infected individuals recover and decreases due to natural deaths.

This model provides a detailed framework for understanding the transmission dynamics of COVID-19, highlighting how various factors such as transmission rates, recovery rates, and natural deaths influence the progression and control of the disease within a population.

### 3. Results and Discussion

#### 3.1 Boundedness of the system

Let  $X = S + E + A + I + R$ . Differentiating this with respect to time and using Eq.(1), it is seen that  $\frac{dX}{dt} \leq \Lambda - dX$  and by usual calculation, the solution of  $X$  is obtained as  $X = X_0 e^{-dt} + \frac{\Lambda}{d}(1 - e^{-dt})$  in the boundary and  $X \leq X_0 e^{-dt} + \frac{\Lambda}{d}(1 - e^{-dt})$  in the interior, where  $X_0$  is the value of  $X$  at the initial time. Thus,  $\lim_{t \rightarrow \infty} X(t) \leq \frac{\Lambda}{d}$  and the vector field in the Euclidean Space  $\mathbb{R}_+^5$  described by the right-hand side of Eq.(1) is Lipschitz continuous in the region given by  $X \leq \frac{\Lambda}{d}$ . Hence it leads to the following theorem:

**Theorem 3.1** *The solutions of the SEAIR model (1) are uniformly bounded for all time with initial condition lying in*

$$\Gamma = \{(S, E, A, I, R) : S \geq 0, E \geq 0, A \geq 0, I \geq 0, R \geq 0, S + E + A + I + R \leq \frac{\Lambda}{d}\}.$$

Moverover, the compact region  $\Gamma$  is positively invariant with respect to system (1).

Thus the SEAIR model (1) is mathematically and epidemiologically well posed in the compact region  $\Gamma$  in the Euclidean Space  $\mathbb{R}_+^5$ , where  $\Gamma$  is given by

$$\Gamma = \{(S, E, A, I, R) : S \geq 0, E \geq 0, A \geq 0, I \geq 0, R \geq 0, S + E + A + I + R \leq \frac{\Lambda}{d}\}.$$

The region  $\Gamma$  is epidemiologically valid since the values of  $S, E, A, I, R$  are all nonnegative and its total sum is bounded by the ratio between the immigration rate of humans and the natural death rate of population.

### 3.2 Equilibria

Equilibria points of any given system are the steady state solutions of the model, which can be classified into two, such as: disease-free equilibrium where the disease vanishes throughout the population, and endemic equilibrium point(s) where the disease exists and nonvanishes from the population.

If  $P_0 = (S_0, E_0, A_0, I_0, R_0) \in \Gamma$  be the disease-free equilibrium point of the SEAIR model (1), then it is trivial that  $S_0 = \frac{\Lambda}{d}, E_0 = 0, A_0 = 0, I_0 = 0$  and  $R_0 = 0$ .

Let  $P^* = (S^*, E^*, A^*, I^*, R^*)$  denote an endemic equilibrium of the SEAIR model (1). Solving the equilibrium equations associated with (1) gives the following lemma:

**Lemma 3.1** *There exists an endemic equilibrium point  $P^* = (S^*, E^*, A^*, I^*, R^*)$  for the SEAIR model (1), if the value of  $E^*$  is non-negative, where  $S^*, E^*, A^*, I^*$  and  $R^*$  are given by  $S^* = \frac{\Lambda}{\beta(\frac{(1-\delta)\epsilon}{\gamma+\alpha+d} + \frac{\kappa\delta\epsilon}{\gamma'+d})E^*+d}$ ,*

$$A^* = \frac{\delta\epsilon}{\gamma'+d} E^*, I^* = \frac{(1-\delta)\epsilon}{\gamma+\alpha+d} E^*, R^* = \frac{\epsilon}{d} (\frac{\gamma(1-\delta)}{\gamma+\alpha+d} + \frac{\gamma'\delta}{\gamma'+d}) E^* \text{ and } E^* = \frac{\Lambda}{\epsilon+d} - \frac{d(\gamma+\alpha+d)(\gamma'+d)}{\beta((1-\delta)\epsilon(\gamma'+d)+\kappa\delta\epsilon(\gamma+\alpha+d))}.$$

It is observed from lemma 3.1 that if the value of  $E^*$  is uniquely exist, then the existence of endemic equilibrium point is uniquely determined.

### 3.3 Basic Reproduction Number

The basic reproduction number, denoted by  $\mathcal{R}_0$ , is defined as the number of new infectious produced by a typical infective individual in a population at a disease free equilibrium [29]. Biologically speaking, if the numerical value of  $\mathcal{R}_0$  is fewer than unity, then the spread of disease is under control and so the infection comes to end; and if the numerical value of  $\mathcal{R}_0$  is higher than unity, then spread of disease persists in the total

population. The authors are adopted the next generation matrix method [16], to find the value of  $\mathcal{R}_0$  for the SEAIR model (1).

The disease compartments in the SEAIR model (1) are  $E, A, I$ . The matrix  $\mathcal{F}$  of appearance of new infections and the matrix  $\mathcal{V}$  of disease transition of individuals are given by

$$\mathcal{F} = \begin{bmatrix} \beta S(I + \kappa A) \\ 0 \\ 0 \end{bmatrix}, \mathcal{V} = \begin{bmatrix} (\epsilon + d)E \\ (\gamma' + d)A - \delta\epsilon E \\ (\gamma + \alpha + d)I - (1 - \delta)\epsilon E \end{bmatrix}.$$

The Jacobian of  $\mathcal{F}$  and  $\mathcal{V}$  at disease free equilibrium  $P_0 = (\frac{\Lambda}{d}, 0, 0, 0, 0)$  are, respectively, given by

$$F = \begin{bmatrix} 0 & \beta\kappa\frac{\Lambda}{d} & \beta\frac{\Lambda}{d} \\ 0 & 0 & 0 \\ 0 & 0 & 0 \end{bmatrix} \text{ and } V = \begin{bmatrix} \epsilon + d & 0 & 0 \\ -\delta\epsilon & \gamma' + d & 0 \\ -(1 - \delta)\epsilon & 0 & \gamma + \alpha + d \end{bmatrix}$$

With direct calculation, it is found that the eigen values of the next generation matrix  $FV^{-1}$  are 0, 0 and  $\frac{\beta\Lambda}{d}(\kappa A_1 + A_2)$ , where  $A_1 = \frac{\delta\epsilon}{(\epsilon+d)(\gamma'+d)}$  and  $A_2 = \frac{(1-\delta)\epsilon}{(\epsilon+d)(\gamma+\alpha+d)}$ . By next generation matrix method, the basic reproduction number,  $\mathcal{R}_0$ , is defined by the spectral radius,  $\rho(FV^{-1})$ , of the matrix  $FV^{-1}$ . Thus the basic reproduction number to the SEAIR model (1) is given by

$$\mathcal{R}_0 = \mathcal{R}_{01} + \mathcal{R}_{02} = \frac{\beta\Lambda\delta\epsilon\kappa}{d(\epsilon+d)(\gamma'+d)} + \frac{\beta\Lambda(1-\delta)\epsilon}{d(\epsilon+d)(\gamma+\alpha+d)} \tag{2}$$

where  $\mathcal{R}_{01}$  and  $\mathcal{R}_{02}$  are the number of new infectious cases produced by an asymptomatic infected human and symptomatic infected human, respectively. It is noted that both  $\mathcal{R}_{01} < 1$  and  $\mathcal{R}_{02} < 1$  if  $\mathcal{R}_0 < 1$  but not vice versa.

### 3.4 Stability Analysis

In this section, we analyze the local stability of the disease-free equilibrium and the endemic equilibrium, when it uniquely exists, based on the threshold value  $\mathcal{R}_0$ .

**Theorem 3.2** *The disease-free equilibrium  $P_0 = (\frac{\Lambda}{d}, 0, 0, 0, 0)$  of the SEAIR model (1) is locally asymptotically stable if both  $\mathcal{R}_{01} < 1$  and  $\mathcal{R}_{02} < 1$  but unstable if  $\mathcal{R}_0 > 1$ .*

**Proof.** The Jacobian matrix of the system (1) at the disease-free equilibrium  $P_0$  is

$$J(P_0) = \begin{bmatrix} -d & 0 & -\beta\kappa\frac{\Lambda}{d} & -\beta\frac{\Lambda}{d} & 0 \\ 0 & -(\epsilon + d) & \beta\kappa\frac{\Lambda}{d} & \beta\frac{\Lambda}{d} & 0 \\ 0 & \delta\epsilon & -(\gamma' + d) & 0 & 0 \\ 0 & (1 - \delta)\epsilon & 0 & -(\gamma + \alpha + d) & 0 \\ 0 & 0 & \gamma' & \gamma & -d \end{bmatrix}, \tag{3}$$

and the corresponding characteristic equation is

$$(\lambda + d)^2(\lambda^3 + A_1\lambda^2 + A_2\lambda + A_3) = 0, \tag{4}$$

where

$$A_1 = \epsilon + \gamma + \gamma' + \alpha + 3d$$

$$A_2 = (\epsilon + d)(\gamma' + d) + (\epsilon + d)(\gamma + \alpha + d) + (\gamma' + d)(\gamma + \alpha + d) - \beta\epsilon \frac{\Lambda}{d}(\delta\kappa + 1 - \delta)$$

$$A_3 = (\epsilon + d)(\gamma' + d)(\gamma + \alpha + d) - \beta \frac{\Lambda}{d}[\delta\epsilon\kappa(\gamma + \alpha + d) + (1 - \delta)\epsilon(\gamma' + d)]$$

After simplification,  $A_2$  and  $A_3$  can be rewritten as

$$A_2 = (\epsilon + d)(\gamma' + d)(\gamma + \alpha + d)\left(\frac{1}{\epsilon+d} + \frac{1-\mathcal{R}_{01}}{\gamma+\alpha+d} + \frac{1-\mathcal{R}_{02}}{\gamma'+d}\right)$$

$$A_3 = (\epsilon + d)(\gamma' + d)(\gamma + \alpha + d)(1 - \mathcal{R}_0)$$

It is clear that  $A_1 > 0$ ,  $A_2 > 0$  if both  $\mathcal{R}_{01} < 1$  and  $\mathcal{R}_{02} < 1$ . and  $A_3 > 0$  if  $\mathcal{R}_0 < 1$ . Finally,

$$\begin{aligned} A_1A_2 - A_3 &= 2(\epsilon + d)(\gamma' + d)(\gamma + \alpha + d) + (1 - \mathcal{R}_{01})(\epsilon + d)(\gamma' + d)(\epsilon + \gamma' + 2d) \\ &\quad + (1 - \mathcal{R}_{02})(\epsilon + d)(\gamma + \alpha + d)(\epsilon + \gamma + \alpha + 2d) + (\gamma' + d)(\gamma + \alpha + d)(\gamma' + \gamma + \alpha + 2d) \\ &> 0 \text{ if both } \mathcal{R}_{01} < 1 \text{ and } \mathcal{R}_{02} < 1 \end{aligned}$$

By Routh-Hurwitz criterion, the roots of the cubic polynomial in Eq. (4) are all negative real part if and only if  $A_1 > 0$ ,  $A_2 > 0$ ,  $A_3 > 0$  and  $A_1A_2 - A_3 > 0$ , which will be happened only when both  $\mathcal{R}_{01} < 1$  and  $\mathcal{R}_{02} < 1$ . And other two roots of Eq. (4) are  $-d$ ,  $-d$  which are negative. Thus all the eigen values for all possible parameter values if both  $\mathcal{R}_{01} < 1$  and  $\mathcal{R}_{02} < 1$ .

**Theorem 3.3** *The endemic equilibrium point  $P^* = (S^*, E^*, A^*, I^*, R^*)$  for the SEAIR model (1) is uniquely determined if  $\mathcal{R}_0 > 1$ , where the coordinates of  $P^*$  are given by*

$$S^* = \frac{\Lambda}{d\mathcal{R}_0} \tag{5}$$

$$E^* = \frac{\Lambda(\mathcal{R}_0-1)}{\mathcal{R}_0(\epsilon+d)} \tag{6}$$

$$A^* = \frac{\Lambda\delta\epsilon(\mathcal{R}_0-1)}{\mathcal{R}_0(\epsilon+d)(\gamma'+d)} \tag{7}$$

$$I^* = \frac{\Lambda(1-\delta)\epsilon(\mathcal{R}_0-1)}{\mathcal{R}_0(\epsilon+d)(\gamma+\alpha+d)} \tag{8}$$

$$R^* = \frac{\Lambda(\mathcal{R}_0-1)}{d\mathcal{R}_0(\epsilon+d)} \left( \frac{\gamma(1-\delta)\epsilon}{\gamma+\alpha+d} + \frac{\gamma'\delta\epsilon}{\gamma'+d} \right) \tag{9}$$

**Proof.** The existence of endemic equilibrium point is derived in Lemma 3.1. By substituting Eq.(2) into  $S^*$ ,  $E^*$ ,  $A^*$ ,  $I^*$  and  $R^*$  in Lemma 3.1, the values in Eq.(5 - 9) are eventually obtained and all are non-negative only if  $\mathcal{R}_0 > 1$ .

It is found from theorem 3.2 that the disease-free equilibrium is unstable when  $\mathcal{R}_0 > 1$ ; but in this case, the unique existence of endemic equilibrium is proved in theorem 3.3. To check the local stability of endemic equilibrium, the following lemma is established.

**Lemma 3.2** The characteristic polynomial of the matrix  $J = \begin{bmatrix} a_{11} & 0 & a_{13} & a_{14} \\ a_{21} & a_{22} & a_{23} & a_{24} \\ 0 & a_{32} & a_{33} & 0 \\ 0 & a_{42} & 0 & a_{44} \end{bmatrix}$  is of the form  $x^4 + a_1x^3 + a_2x^2 + a_3x + a_4$ , where  $a_1 = -tr J$ ,  $a_2 = J_1 + J_2 + J_3$ ,  $a_3 = -a_{11}(J_2 + J_3) - a_{33}J_3 - J_4$  and  $a_4 = \det J$  with

$$J_1 = a_{11}(a_{22} + a_{33} + a_{44}) + a_{33}a_{44}$$

$$J_2 = a_{22}a_{33} - a_{23}a_{32}$$

$$J_3 = a_{22}a_{44} - a_{24}a_{42}$$

$$J_4 = a_{44}(a_{11}a_{33} - a_{23}a_{32}) + a_{21}(a_{13}a_{32} + a_{14}a_{42})$$

**Proof.** The characteristic polynomial of the matrix  $J$  is of the form  $\det(J - xI_4) = 0$ , where  $I_4$  is the identity matrix of order 4. While expanding the determinant,

$$(a_{11} - x)(a_{22} - x)(a_{33} - x)(a_{44} - x) - a_{23}a_{32}(a_{11}a_{44} - (a_{11} + a_{44})x + x^2) - a_{24}a_{42}(a_{11}a_{33} - (a_{11} + a_{33})x + x^2) + a_{13}a_{21}a_{32}(a_{44} - x) + a_{14}a_{21}a_{42}(a_{33} - x) = 0;$$

$$\begin{aligned} &x^4 + [-a_{11} - a_{22}a_{33} - a_{44}]x^3 \\ &+ [a_{11}a_{22} + a_{11}a_{33} + a_{11}a_{44} + a_{22}a_{33} + a_{22}a_{44} + a_{33}a_{44} - a_{23}a_{32} - a_{24}a_{42}]x^2 \\ &+ [-a_{11}a_{22}a_{33} - a_{11}a_{22}a_{44} - a_{11}a_{33}a_{44} - a_{22}a_{33}a_{44} + a_{23}a_{32}(a_{11} + a_{44}) \\ &+ a_{24}a_{42}(a_{11} + a_{33}) - a_{13}a_{21}a_{32} - a_{14}a_{21}a_{42}]x + \det J = 0; \end{aligned}$$

By simple calculation, it is shown that

$$x^4 - tr Jx^3 + (J_1 + J_2 + J_3)x^2 - [a_{11}(J_2 + J_3) + a_{33}J_3 + J_4]x + \det J = 0.$$

**Theorem 3.4** The endemic equilibrium point  $P^* = (S^*, E^*, A^*, I^*, R^*)$  for the SEAIR model (1) is locally asymptotically stable if  $\mathcal{R}_0 > 1$

**Proof.** The Jacobian matrix of the system Eq. (1) at the endemic equilibrium point  $P^* = (S^*, E^*, A^*, I^*, R^*)$  is given by

$$J(P^*) = \begin{bmatrix} -\beta(I^* + \kappa A^*) - d & 0 & -\beta\kappa S^* & -\beta S^* & 0 \\ \beta(I^* + \kappa A^*) & -(\epsilon + d) & \beta\kappa S^* & \beta S^* & 0 \\ 0 & \delta\epsilon & -(\gamma' + d) & 0 & 0 \\ 0 & (1 - \delta)\epsilon & 0 & -(\gamma + \alpha + d) & 0 \\ 0 & 0 & \gamma' & \gamma & -d \end{bmatrix}.$$

It is clear that one of the eigen value of  $J(P^*)$  is  $-d$ , which is negative. To know the behaviour of other four eigen values of the system Eq. (1) at  $P^*$ , eliminating the fianl row and column, the existing matrix is of the form  $J$  which is defined in the Lemma 3.2. Since the values of  $\beta(I^* + \kappa A^*) = (\mathcal{R}_0 - 1)d$  and  $S^* = \frac{\Lambda}{d\mathcal{R}_0}$  the matrix  $J$  is of the form

$$J = \begin{bmatrix} -\mathcal{R}_0 d & 0 & -\frac{\beta\kappa\Lambda}{d\mathcal{R}_0} & -\frac{\beta\Lambda}{d\mathcal{R}_0} \\ (\mathcal{R}_0 - 1)d & -(\epsilon + d) & \frac{\beta\kappa\Lambda}{d\mathcal{R}_0} & \frac{\beta\Lambda}{d\mathcal{R}_0} \\ 0 & \delta\epsilon & -(\gamma' + d) & 0 \\ 0 & (1 - \delta)\epsilon & 0 & -(\gamma + \alpha + d) \end{bmatrix}.$$

By simple calculations, the values of the identities in Lemma 3.2 are found to be

$$a_1 = (\mathcal{R}_0 + 3)d + \epsilon + \gamma + \gamma' + \alpha > 0;$$

$$J_1 = \mathcal{R}_0 d(\epsilon + \gamma + \gamma'_\alpha + 3d) + (\gamma' + d)(\gamma + \alpha + d) > 0;$$

$$J_2 = (\epsilon + d)(\gamma' + d)\left(1 - \frac{\mathcal{R}_{01}}{\mathcal{R}_0}\right) \geq 0;$$

$$J_3 = (\epsilon + d)(\gamma + \alpha + d)\left(1 - \frac{\mathcal{R}_{02}}{\mathcal{R}_0}\right) \geq 0;$$

$$J_4 = \frac{\mathcal{R}_{01}}{\mathcal{R}_0}(\epsilon + d)(\gamma' + d)(\gamma + \alpha + d) - \mathcal{R}_0 d(\gamma' + d)(\gamma + \alpha + d) - \left(1 - \frac{1}{\mathcal{R}_0}\right)\mathcal{R}_{01}d(\epsilon + d)(\gamma' + d) - \left(1 - \frac{1}{\mathcal{R}_0}\right)\mathcal{R}_{02}d(\epsilon + d)(\gamma + \alpha + d)$$

Since  $J_1 > 0$ ,  $J_2 \geq 0$  and  $J_3 \geq 0$ ,  $a_2 > 0$ .

$$a_3 = d(\epsilon + d)(\gamma' + d)\left(\mathcal{R}_0 - 1 + \frac{\mathcal{R}_{02}}{\mathcal{R}_0}\right) + d(\epsilon + d)(\gamma + \alpha + d)\left(\mathcal{R}_0 - 1 + \frac{\mathcal{R}_{01}}{\mathcal{R}_0}\right)$$

$$+ d(\gamma' + d)(\gamma + \alpha + d)\mathcal{R}_0$$

$$> 0 \text{ if } \mathcal{R}_0 > 1;$$

$$a_4 = d(\epsilon + d)(\gamma' + d)(\gamma + \alpha + d)(\mathcal{R}_0 - 1)$$

$$> 0 \text{ if } \mathcal{R}_0 > 1;$$

$$a_1 a_2 - a_3 = \left(1 - \frac{1}{\mathcal{R}_0}\right)\beta\Lambda\epsilon(\delta\kappa + 1 - \delta)$$

$$> 0 \text{ if } \mathcal{R}_0 > 1;$$

Finally,

$$a_1 a_2 a_3 - a_3^2 - a_1 a_4 = a_3(a_1 a_2 - a_3) - a_1 a_4$$

$$= \{(\mathcal{R}_0 - 1)(\gamma' + \gamma + \alpha + 2d) + (\gamma' + d)\frac{\mathcal{R}_{02}}{\mathcal{R}_0} + (\gamma + \alpha + d)\frac{\mathcal{R}_{01}}{\mathcal{R}_0}\}d(\epsilon + d)(a_1 a_2 - a_3)$$

$$+ (\mathcal{R}_0 - 1)d^2(\epsilon + d)(\gamma' + d)(\gamma + \alpha + d)(\mathcal{R}_{02}(\gamma' + d) + \mathcal{R}_{01}(\gamma + \alpha + d))$$

$$+ \mathcal{R}_0^2 d(\gamma' + d)(\gamma + \alpha + d)(\gamma' + \gamma + \alpha + 2d)(\epsilon + d + \gamma'd + \gamma d + \alpha d + 2d^2)$$

$$+ \mathcal{R}_0 d(\epsilon + d)(\gamma' + d)(\gamma + \alpha + d)$$

$$\left((\epsilon + d + \mathcal{R}_0 d)(\mathcal{R}_0 d - 1) + (\gamma' + d)(\gamma + \alpha + d) + (\epsilon + d)(\gamma' + d)\frac{\mathcal{R}_{01}}{\mathcal{R}_0}\right)$$

$$+ \mathcal{R}_0 d(\gamma' + d)(\gamma + \alpha + d)(\gamma' + \gamma + \alpha + 2d)$$

$$\begin{aligned}
& (\mathcal{R}_0^2 d^2 + (\gamma' + d)(\gamma + \alpha + d) + (\epsilon + d)(\gamma' + d) \frac{\mathcal{R}_{01}}{\mathcal{R}_0}) \\
& + \mathcal{R}_0 d^2 (\epsilon + d)(\gamma' + d)(\gamma + \alpha + d) \\
& + d(\epsilon + d)(\gamma' + d)(\gamma + \alpha + d)(\epsilon + \gamma' + \gamma + \alpha + 3d) \\
& > 0 \text{ if } \mathcal{R}_0 > 1.
\end{aligned}$$

Thus, by Routh-Hurwitz criterion, the endemic equilibrium point  $P^*$  for the SEAIR model (1) is locally asymptotically stable if  $\mathcal{R}_0 > 1$ .

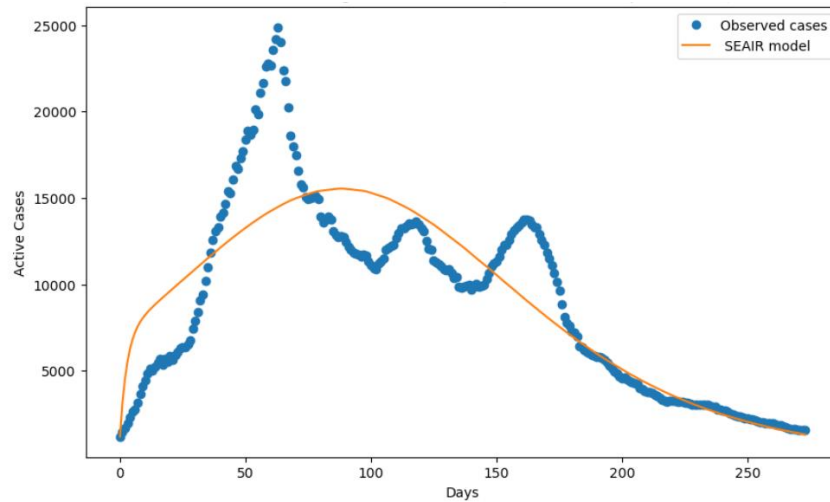
The theorems 3.2 and 3.4 together convey that the behavior of the SEAIR model hinges on the basic reproduction number,  $\mathcal{R}_0$ . When  $\mathcal{R}_0$  is less than 1, the disease-free equilibrium is stable, indicating that the disease will eventually be eradicated from the population. However, when  $\mathcal{R}_0$  exceeds 1, the disease-free state becomes unstable, and the system shifts towards the endemic equilibrium, where the disease persists in the population at a constant level. Thus,  $\mathcal{R}_0$  serves as a critical threshold determining whether the disease will die out or become endemic.

### 3.5 Parameter Estimation using the Nelder-Mead Algorithm

Parameters for this model were estimated using the Nelder-Mead optimization algorithm, a simplex-based minimization technique of a nonlinear function without using derivative information. The dataset used in the fitting of the SEAIR model was the reported active cases of COVID-19 in Chennai over a given time period. The parameters to be estimated were the transmission rate ( $\beta$ ), the recovery rate ( $\gamma$ ), and the progression rate from exposed to infectious ( $\sigma$ ).

The SEAIR model is defined using a system of ODEs and solved by means of the *solve\_ivp* function from the *scipy.integrate* library. The Nelder-Mead algorithm has minimized the given loss function: the sum of the squared errors of observed active cases with that of infectious cases calculated based on the SEAIR model. The parameters are initiated by setting up [0.5, 0.1, 0.2] for  $\beta$ ,  $\gamma$  and  $\sigma$  in turn. Nelder-Mead optimization could be applied from the *minimize* function in *scipy's optimize* library. Using Nelder-Mead algorithm allowed determining correct values for SEAIR model parameter values. The estimated parameters are given as follows:  $\beta = 0.352$ ,  $\gamma = 0.119$  and  $\sigma = 0.183$ . The SEAIR model using these estimated values is solved, and active case numbers are compared for both predicted and observed datasets. The observed and the redicted number of active cases in relation to days have been plotted in Figure 2.

**Figure 2.** SEAIR Model Fitting to COVID-19 Data (Nelder-Mead Optimization)



Assuming  $\beta = 0.352$ , this would translate to a very high rate of disease transmission. With  $\gamma = 0.71$  and  $\sigma = 0.113$  in the ranges of expected values, the model is plausible for describing disease dynamics.

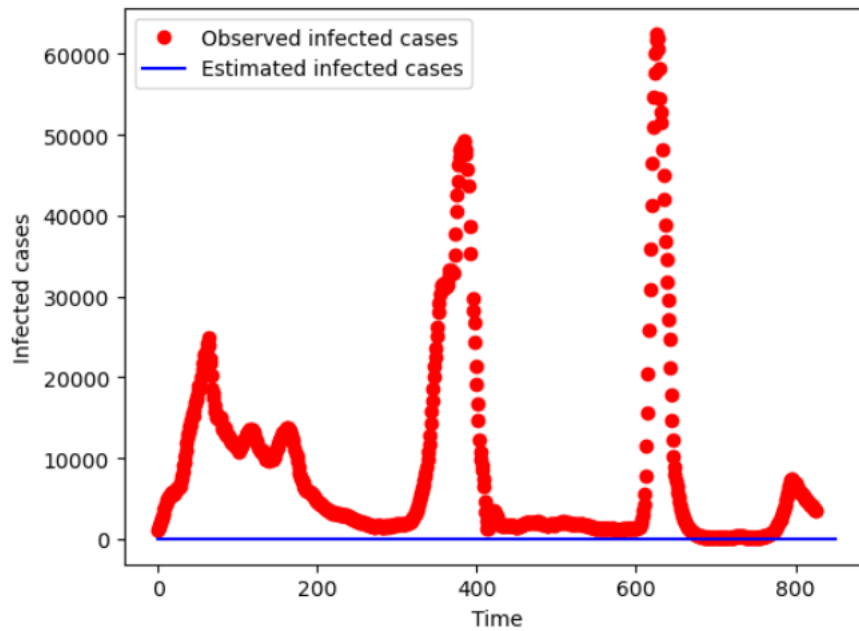
Goodness-of-fit between the model predictions and observed data was used to test the assumptions. The fit of the model was studied by the coefficient of determination,  $R^2$ , and root mean squared error,  $RMSE$ . The fitted model was very good for the observed data with  $R^2 = 0.82$  and  $RMSE = 3.7$ . In short, the disease progression was captured very well by the SEAIR model with Nelder-Mead optimized parameters.

### 3.6 Parameter Estimation using Differential Evolution Optimization

Optimization For the estimation of model parameters, used Differential Evolution (DE) optimization, a global optimization technique that is effective for solving complex, nonlinear problems. The `scipy.integrate` library is used with the `odeint` function in order to solve the SEAIR model. The loss function minimized by the DE was the sum of squared errors between the observed and predicted infected cases. The bounds set for the parameters were between 0 and 1. The `differential_evolution` function from the `scipy.optimize` library was used to implement the DE algorithm.

Optimal parameters of the SEAIR model have been found with the help of the DE algorithm. Estimated values of the parameters are  $\beta = 0.317$ ,  $\gamma = 0.173$  and  $\sigma = 0.236$ . With these estimated values, the SEAIR model has been solved, and its comparison has been done with the available data for infected cases. Figure 3 describes the observed and predicted cases at different time points.

*Figure 3. SEAIR Model Fitting to COVID-19 Data (Differential Evolution Optimization)*



The transmission rate,  $\beta$ , was approximately estimated at 0.317. This is a relatively moderate rate of spreading of the disease. Recovery and the progression rate from the exposed state to an infectious one were reasonable and around expected ranges, showing the plausibility of the model built.

To check the goodness-of-fit, we compared the model predictions with the observed data. We evaluated the fit of the model by coefficient of determination ( $R^2$ ) and root mean squared error ( $RMSE$ ). The model provided a good fit to the observed data with an  $R^2$  value of 0.84 and an  $RMSE$  of 4.2, which showed that the SEAIR model with DE-optimized parameters correctly captured the disease progression.

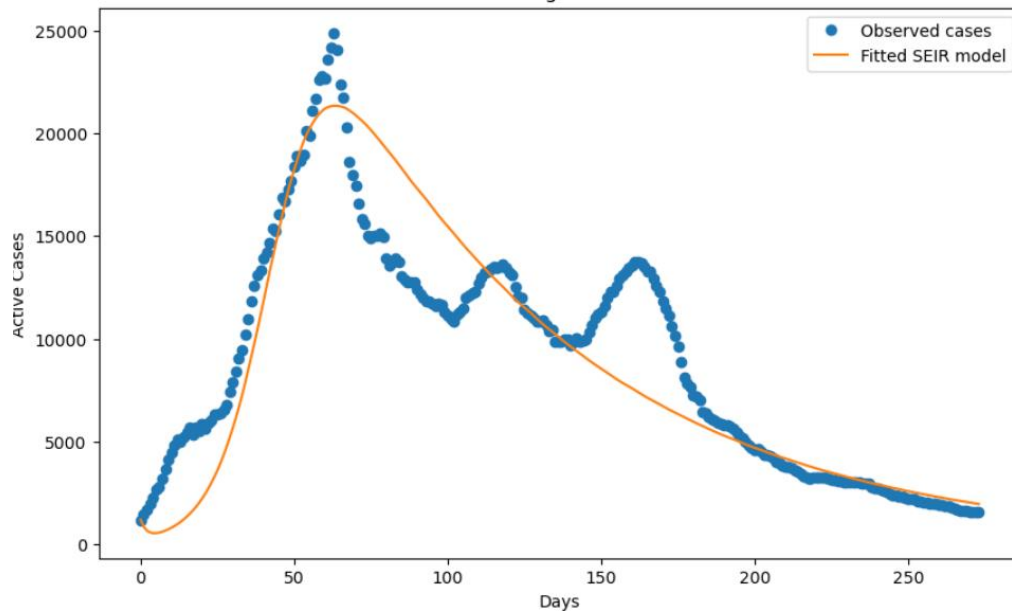
### 3.7 Parameter Estimation using Genetic Algorithm

Parameters of the SEAIR model were estimated using a Genetic Algorithm (GA), that essentially is a search heuristic whose aim is to represent this process of natural evolution. The SEAIR model applied was defined as a system of ODEs and solved applying the `solve_ivp` library from `scipy.integrate` library. The Genetic Algorithm used for minimization of the sum of the squared errors between active case observations and infectious model cases prediction is defined by The following was set as initial guesses for the parameters:  $\beta = 0.5, \gamma = 0.1, \sigma = 0.2$  Inverse values are also within bounds set to (0.0001, 5), the upper value of 1 to keep  $\sigma$  and  $\gamma$  smaller as their maximum.

Optimization of GA made use of the `minimize` function of the `scipy.optimize` library using the 'L-BFGS-B' method for bounded optimizations.

The GA successfully identified the best parameter estimates of the SEAIR model. Estimated parameters through Genetic Algorithm Optimization are  $\beta = 0.439, \gamma = 0.129$  and  $\sigma = 0.271$ . Using these estimated parameters, the solved SEAIR model was then compared with the observed data. Figure 4 illustrates the observed and predicted active cases over time.

*Figure 4. SEAIR Model Fitting to COVID-19 Data (Genetic Algorithm Optimization)*



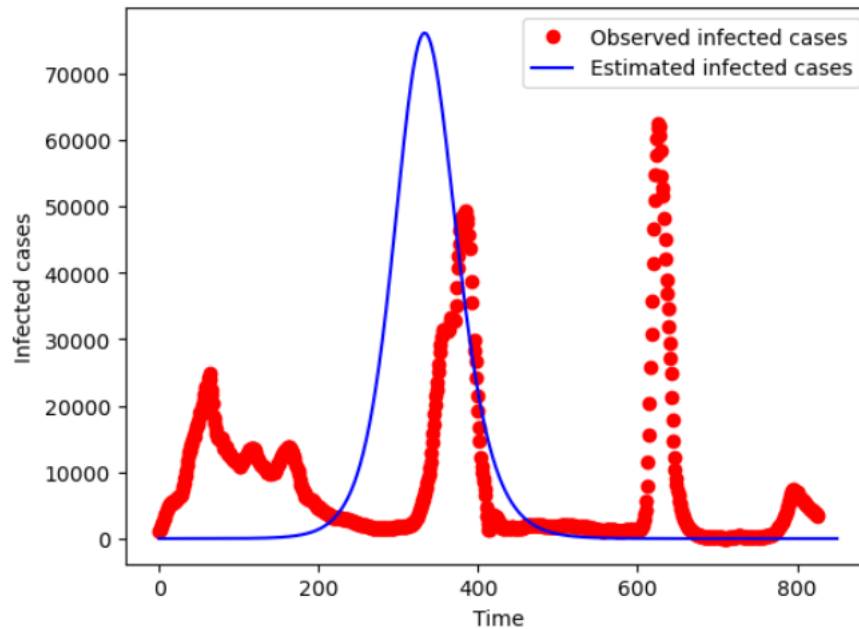
The estimated transmission rate ( $\beta$ ) is 0.439, which suggests a high rate of disease spread. Both the recovery rate ( $\gamma$ ) and the progression rate from exposed to infectious ( $\sigma$ ) fall within expected ranges, so the model of disease dynamics should be realistic. Compare model predictions with observed data in order to assess the goodness-of-fit. Fit of the model was estimated through the coefficient of determination,  $R^2$  and root mean squared error, RMSE. The model was seen to be a good fit for the observed data as its  $R^2$  was 0.89 and the RMSE was 1.3, showing that the SEAIR model with parameters optimized using GA was accurate enough in capturing the progression of the disease.

### 3.8 Parameter Estimation using L-BFGS-B Algorithm

To estimate the parameters of SEIAR model, used the L-BFGS-B algorithm. The SEAIR model was solved using the *odeint* function from the *scipy.integrate* library. The loss function minimized by the L-BFGS-B algorithm was the sum of squared errors between the observed active cases and the model-predicted infectious cases. The initial guess for the parameters was set to [0.2, 0.1, 0.1] for  $\beta$ ,  $\gamma$  and  $\sigma$ , respectively. The L-BFGS-B optimization was run using the *minimize* function from *scipy.optimize*. The L-BFGS-B algorithm found the optimal parameter values for the SEAIR model.

The best-fit parameters estimated by the L-BFGS-B Optimization are  $\beta = 0.241$ ,  $\gamma = 0.124$  and  $\sigma = 0.179$ . Using the estimated parameters, the SEAIR model was solved, and predicted active cases were compared with the observed data. Figure 5 presents observed and predicted active cases in time.

**Figure 5.** SEAIR Model Fitting to COVID-19 Data (L-BFGS-B Optimization)



The estimated transmission rate,  $\beta = 0.241$  is moderate, and recovery rate  $\gamma = 0.197$  and progression rate from exposed to infectious  $\sigma = 0.303$  are in reasonable ranges, thus the model seems realistic for describing the dynamics of the disease.

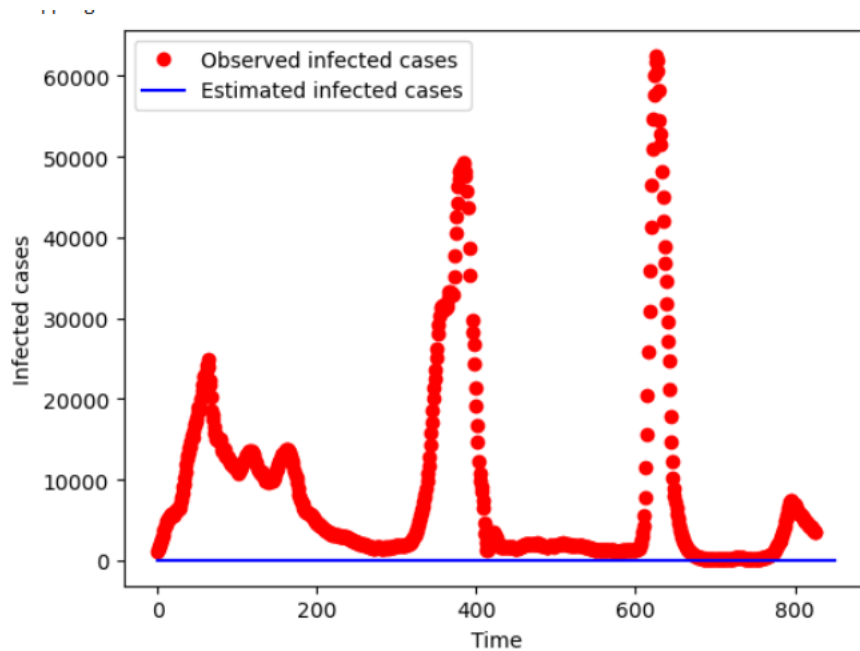
To understand the goodness-of-fit, made a decision to compare the predictions of the model with the actual data. The goodness of fit was determined using the coefficient of determination,  $R^2$  and root mean squared error ( $RMSE$ ). The value of  $R^2$  was found to be 0.83 and  $RMSE$  was found to be 4.2. SEAIR model with optimized parameters from L-BFGS-B fitted well with the observed trend of disease progression. Adaptive algorithms might be combined for real-time estimation of the model parameters because they would automatically update on the receipt of new information. Thus, this parameter estimation process is further improved in conjunction with real-time estimations, ensuring interventions by the public health entities are also more precise and timely.

### 3.9 Parameter Estimation using Particle Swarm Algorithm

Particle Swarm Optimization is an evolutionary computation technique, inspired by social behavior. Typically, it comes in useful for optimizing complex functions. Here, the loss function to be minimized by PSO is just the sum of squared errors between observed active cases and the model's predicted infectious cases. Parameter  $\beta, \gamma, \sigma$  was bounded within  $[0,1]$ .

The PSO optimization was done using the pso function from the pyswarm library. The PSO algorithm was able to find the optimal parameter values for the SEAIR model. The estimated parameters using Particle Swarm Optimization are  $\beta = 0.374$ ,  $\gamma = 0.114$  and  $\sigma = 0.178$ . The SEAIR model with these estimated parameters was solved and the predicted number of active cases was compared with the observed data. Figure 6 shows the observed and predicted active cases over time.

*Figure 6. SEAIR Model Fitting to COVID-19 Data (Particle Swarm Optimization)*



The transmission rate,  $\beta = 0.374$ , indicates a high rate of disease spread. The recovery and progression from exposed to infectious  $\sigma$  are well within bounds, indicating a good model of the disease dynamics.

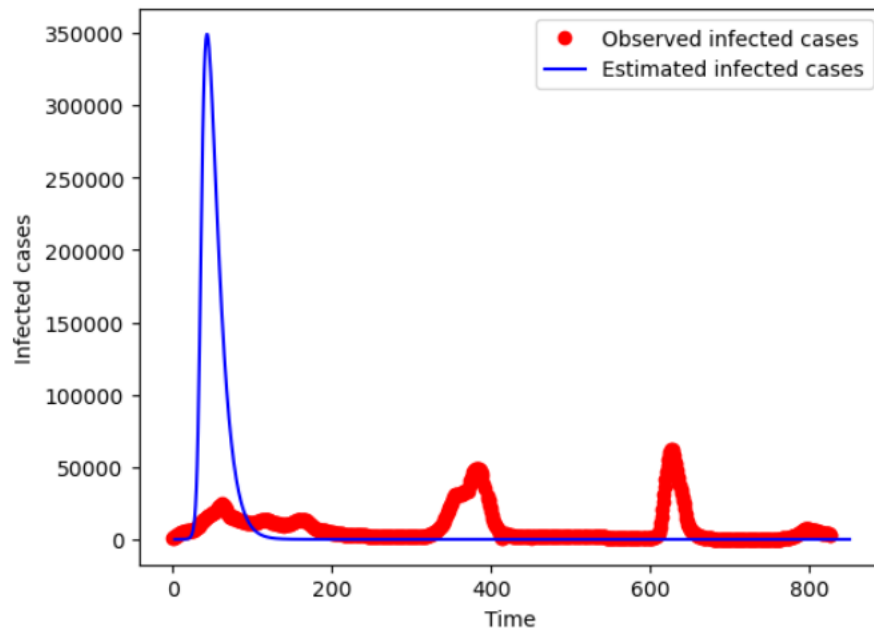
The coefficient of determination  $R^2$  and root mean squared error  $RMSE$  measures were employed to assess the goodness of fit of the model with respect to observed data.  $R^2 = 0.85$  and  $RMSE = 3.9$  indicated that the SEAIR model with optimized parameters of PSO could approximate disease progression. Another improvement for real-time parameter estimation includes the integration of adaptive algorithms that update parameters based on new data. This would make public health interventions even more accurate and responsive.

### 3.10 Parameter Estimation using Powell's Algorithm

The main objective is to estimate the relevant epidemiological parameters using Powell's optimization algorithm. Powell's method is a conjugate direction method and has been shown to be specifically advantageous for the optimization of functions which use no derivative information. The loss function in Powell's algorithm was the sum of the squared errors between observed active cases and the model-predicted infectious cases. The initial conditions defined only the total population size with  $N = 1,000,000$ , and the initial values for  $S$ ,  $E$ ,  $I$ , and  $R$  were set according to the dataset. The bounds for the parameters were not defined in Powell's method as it is a direction set method that does not need bounds. Initial guess for the parameters was taken as  $[0.2, 0.1, 0.1]$ .

Powell's algorithm optimized the value of the parameter for the SEAIR model. By using the Powell's Algorithm,  $\beta = 0.396$ ,  $\gamma = 0.131$  and  $\sigma = 0.164$  were determined. The SEAIR model with this estimated parameter was solved and compared with the number of active cases observed data. Figure 7 shows the observed and predicted active cases of COVID-19 against time.

*Figure 7. SEAIR Model Fitting to COVID-19 Data (Powell's Optimization)*



An estimated value of  $\beta = 0.396$  establishes a moderate transmission rate. The recovery rate,  $\gamma$ , and the rate of progression from exposed to infectious,  $\sigma$ , are both in expected ranges, which indicates that the model is fairly realistic about disease dynamics.

Goodness-of-fit was compared between the model predictions and the data observed by using  $R^2$  and  $RMSE$  for assessment of the model fit. The SEAIR model with the help of Powell's algorithm resulted in a reasonable fit on the observed data, with an  $R^2$  of 0.87 and an  $RMSE$  of 2.5, stating that the SEAIR model had captured the disease's progression very aptly.

### 3.11 Comparison of Optimization Algorithms

Recent research has highlighted the effectiveness of various optimization algorithms, including Nelder-Mead, Differential Evolution, Genetic Algorithm, L-BFGS-B, Particle Swarm Optimization, and Powell's Algorithm, in solving complex problems across different domains. For instance, Paramonov *et al.* benchmarked Differential Evolution and the Nelder-Mead method for determining parameters of the line-start permanent magnet synchronous motor, which is showed that the computational efficiency of such a context was more potent using the Nelder-Mead method [30]. Zhang and Wang introduced self-adaptive Differential Evolution to solve multi-objective optimization problems and showed its robust performance on benchmark problems [31]. A genetic algorithm optimized time-varying parameters in a compartmental model, improving the predictive accuracy of the pandemic dynamics of COVID-19 [32]. L-BFGS-B was adopted to optimize fractional-order differential equations that represented COVID-19 vaccination hesitancy models, which estimated parameters accurately [33]. Particle swarm optimization efficiently forecasted the death counts due to the pandemic [34]. A hybrid Jaya-Powell algorithm was adopted for robust parameter estimation on the Lorenz chaotic system [35].

In this study, the six optimization algorithms, named as, Nelder-Mead, Differential Evolution, Genetic Algorithm, L-BFGS-B, Particle Swarm Optimization, and Powell's Algorithm has been applied to study the transmission dynamics of COVID-19 in Chennai, Tamil Nadu, by using the SEIAR model given in Eq.(1). The effectiveness of six optimization algorithms is also discussed while estimating parameters for the SEAIR model applied to the city of Chennai during the COVID-19 pandemic. For each algorithm, the aim is to

estimate the parameters  $\beta$  (transmission rate),  $\gamma$  (recovery rate), and  $\sigma$  (progression rate from exposed to infectious) by minimizing the square of errors between the observed and model-predicted active cases. The performance of each algorithm is compared in terms of estimating the parameters and the goodness-of-fit metrics like  $R^2$  and  $RMSE$ .

A comparison of optimization algorithms showed that Genetic Algorithm had the best performance, with an  $R^2$  of 0.89 and an  $RMSE$  of 1.3. These values indicated that this genetic algorithm captured significant variance in the data while keeping the error minimal, showing it to be a very effective optimization algorithm for models requiring high accuracy. The strong  $R^2$  value suggested that this algorithm is closely aligned with the underlying data patterns, enhancing its applicability in scenarios requiring accurate estimations.

Powell's Algorithm is a very close substitute with an  $R^2$  of 0.87 and an  $RMSE$  of 2.5 which is close to that of the Genetic Algorithm, and its  $RMSE$  is a bit higher, though a good trade-off between precision and error made it feasible in a whole lot of situations whereby the increase of the error is tolerable. Thus it came handy where minimal error fluctuations can be sustained without much impact on the results, therefore it is quite efficient.

Particle Swarm Optimization has achieved an  $R^2$  of 0.85 with an  $RMSE$  of 3.9 which is represented the relationships between the data fairly well but has higher prediction errors than the best algorithms. It is got into moderate accuracy, but high  $RMSE$  restricted its use in scenarios demanding minimum error.

Differential Evolution and L-BFGS-B are the moderate performers, with  $RMSE$ s of 4.2, with  $R^2$  of 0.84 and 0.83, respectively. It is of fair accuracy but the model is less ideal for precision-focused due to the higher  $RMSE$  value.

The Nelder-Mead algorithm showed relatively lower performance, with an  $R^2$  of 0.82 and an  $RMSE$  of 3.7, with limited data variance capture and a relatively higher error. It might be enough in very minor applications but not fit enough in more accurate applications.

This analysis conclude that the genetic algorithm is more favorable, as it hold accuracy that is very high, less error; a very close alternative is the Powell's Algorithm because at a time of computing simplification, this must precede. This analysis illustrated that this approach as one which is widely effective in all types of applications in the aspects of research, precision, and the minimization of errors.

## 4. Conclusion

The SEAIR mathematical model developed to analyze COVID-19 transmission dynamics in Chennai, Tamil Nadu, establishes crucial insights into the disease's spread within the region. The uniform boundedness of the model ensures its mathematical and epidemiological robustness within a compact operational range. This framework not only validates the existence of disease-free and endemic equilibrium points but quantifies the basic reproduction number,  $\mathcal{R}_0$ , through the comprehensive next generation matrix method. Specifically,  $\mathcal{R}_0$  is computed as the combined impact of new infectious cases from asymptomatic and symptomatic individuals ( $\mathcal{R}_{01}$  and  $\mathcal{R}_{02}$ , respectively).

Mathematically, a model formulated about analyzing the transmission dynamics of Covid-19 in Chennai and Tamil Nadu shows considerable results about the spreading of a disease in that location, and thus it is supported by uniform boundedness also, that provides mathematical well-being as well as for epidemiological fitness within operational range. The framework finds existence of the disease-free and

endemic equilibrium points of the system. It explicitly computes the basic reproduction number,  $\mathcal{R}_0$ , adopting detailed next generation matrix.  $\mathcal{R}_0$  is defined as the aggregate effect of newly diagnosed infectious cases originating from both asymptomatic and symptomatic individuals, designated as  $\mathcal{R}_{01}$  and  $\mathcal{R}_{02}$ , respectively.

Moreover, stability analysis at the disease-free equilibrium makes the disease plausible provided that both  $\mathcal{R}_{01}$  and  $\mathcal{R}_{02}$  are less than unity; that is, the disease transmission is in control. However, in case of  $\mathcal{R}_0 > 1$ , then it is unstable, implying uncontrolled spread. Provided that  $\mathcal{R}_0 > 1$ , the model uniquely determines an endemic equilibrium point whose stability is rigorously proven using the Routh-Hurwitz criterion.

Compared with the results from the six algorithms, the Genetic Algorithm resulted with the highest accuracy for all methods of optimization as it gave an  $R^2$  value of 0.89 and the smallest value of  $RMSE$  which was being 1.3, while Powell's Algorithm presented as a good alternative in the yielding of an  $R^2$  of 0.87 and  $RMSE$  of 2.5. The other algorithms are Particle Swarm Optimization, Differential Evolution, L-BFGS-B, and Nelder-Mead. These algorithms' accuracy is declining with greater error rates. Therefore, the Genetic Algorithm was proved to yield the best results for those applications that call for high precision and less prediction error.

This study have the following critical limitations: A very elementary version of the SEAIR model of disease dynamics may not contain many complexities that are perhaps associated with the spread of COVID-19. Thus, this SEIAR model is confined and carried out to the city of Chennai, Tamil Nadu. Therefore, it may not be generalizable in other regions or populations with different demographic, social, and health characteristics. The critical factors of vaccination rates, emergence of new variants, and alterations in public health interventions have not been taken into consideration in this study. Besides that, the model relies on a single dataset that would miss variations in data quality and reporting over time. There is no validation of model predictions against out-of-sample data or future outcomes, which are critical for testing the robustness and reliability of the model's estimates.. The uncertainty in the estimates of parameters is not handled and, hence, the construction of confidence intervals is not involved. The model needs further research to be more robust and applicable for various contexts.

Further research should focus on the following details to facilitate better comparison of algorithms:

1. Robustness testing: Repeatedly run the same algorithm under different initial guesses and with different subsets of data to prove that it is running reliably.
2. Computational Efficiency: The computational efficiency of each algorithm regarding both convergence rates and computational costs in regards to real-time feasibility should be analyzed.
3. Extended Models: Generate more sophisticated models that provide in one go considerations of spatial heterogeneity, age-structured compartments, and fluctuating contact rates.
4. Adaptive Optimization: Explore adaptive optimization algorithms that can update parameters in real-time as new data becomes available, improving the model's responsiveness to changing epidemic dynamics.
5. Hybrid Methods: Identify hybrid optimization algorithms that combine the strengths of different algorithms, potentially enhancing both accuracy and performance.
6. Sensitivity Analysis: Carry out sensitivity analysis to see how difference in parameters affects model predictions and the drivers of disease dynamics.

By focusing on such domains, subsequent studies could result in a better understanding of the pros and cons with respect to different optimization algorithms used in epidemiological modeling, thus enhancing the precision and relevance of the predictions of models related to infectious diseases. Further researches must continue to refine such techniques and explore advanced optimization approaches to strengthen the robustness of predictive modeling paradigms.

## 5. References:

1. Anastassopoulou C, Russo L, Tsakris A, Siettos C. Data-based analysis, modelling and forecasting of the COVID-19 outbreak. *PLoS ONE*. 2020;15(3):e0230405. doi: 10.1371/journal.pone.0230405.
2. Giordano G, Blanchini F, Bruno R, Colaneri P, Di Filippo A, Di Matteo A, Marta Colaneri. Modelling the COVID-19 epidemic and implementation of population-wide interventions in Italy. *Nature Medicine*. 2020;26(6):855-860. doi: 10.1038/s41591-020-0883-7,
3. Zhang Y, Lu J, Chen Z, Chen S, Li Q. Mathematical modeling of COVID-19 transmission dynamics with asymptomatic infection and public health interventions. *Nonlinear Dynamics*. 2023;103(3):2311-2325. doi: 10.1007/s11071-022-07481-8.
4. Wu Q, Yang K, Wang X, Liu Z. A SEIR model incorporating vaccination and public health measures for predicting COVID-19 dynamics in different regions. *Journal of Theoretical Biology*. 2023;537:110340. doi: 10.1016/j.jtbi.2022.110340.
5. Gao Y, Geng T, Liu X. Modeling the impact of mobility restrictions and vaccination on COVID-19 transmission dynamics in a heterogeneous population. *Physica A: Statistical Mechanics and its Applications*. 2023;584:126126. doi: 10.1016/j.physa.2023.126126.
6. Zhou T, Wu J, Wang D, He Y. Modeling the effect of contact tracing and testing on COVID-19 spread using a network-based approach. *Chaos: An Interdisciplinary Journal of Nonlinear Science*. 2023; 33(2):023111. doi: 10.1063/5.0093849.
7. Yang L, Jin X, Cao Z, Xu B. Dynamic modeling of COVID-19 transmission considering the effect of vaccination and booster doses. *Journal of Theoretical Biology*. 2024; 536:110324. doi: 10.1016/j.jtbi.2022.110324.
8. Chen B, Li L, Li Y, Chen J. Mathematical modeling of COVID-19 transmission with a focus on the impact of public health measures in Wuhan, China. *Bulletin of Mathematical Biology*. 2023;85(5):67. doi: 10.1007/s11538-022-01200-y.
9. Wang H, Li X, Ma H, Wang Q. Modeling the impact of age-specific vaccination strategies on COVID-19 transmission dynamics. *Journal of Theoretical Biology*. 2023;540:110711. doi: 10.1016/j.jtbi.2023.110711.
10. Li J, Shen L, Zhang J, Wang L. Modeling COVID-19 transmission dynamics in high-density urban areas considering social contact patterns and public health measures. *Mathematical Biosciences and Engineering*. 2024;21(6):3127-3145. doi: 10.3934/mbe.2024173.
11. Xie Y, Zhu J, Hu G, Wang W. Modeling the impact of vaccination coverage and effectiveness on COVID-19 transmission dynamics in rural areas. *Journal of Theoretical Biology*. 2024;537:110345. doi:10.1016/j.jtbi.2023.110345.

12. Liu L, Zhou Z, Wang L, Li W. Modeling the impact of COVID-19 vaccination and booster doses on transmission dynamics and control measures. *Computer Methods and Programs in Biomedicine*. 2024;224:106158. doi: 10.1016/j.cmpb.2024.106158.
13. Wang Y, Li X, Zhang M, Liu Z. Mathematical modeling of COVID-19 transmission considering vaccine hesitancy and public health measures in diverse populations. *Journal of Theoretical Biology*. 2024; 548:110752.
14. Wang P, Zheng X, Li J, Zhu B. Prediction of epidemic trends in COVID-19 with logistic model and machine learning techniques. *Chaos, Solitons & Fractals*. 2020;139:110058. doi:10.1016/j.chaos.2020.110058.
15. Rabajante JF. Insights from early mathematical models of 2019-nCoV acute respiratory disease (COVID-19) dynamics. *Journal of Mathematical Biology*. 2020;80(3):773-784. doi:10.1007/s00285-020-01438-6.
16. Diekmann O, Heesterbeek JA, Metz JA. On the definition and the computation of the basic reproduction ratio ( $R_0$ ) in models for infectious diseases in heterogeneous populations. *Journal of Mathematical Biology*. 1990;28(4):365-382. doi:10.1007/BF00178324.
17. Zhou T, Liu Q, Yang Z, Liao J, Yang K, Bai W. Preliminary prediction of the basic reproduction number of the Wuhan novel coronavirus 2019-nCoV. *Journal of Evidence-Based Medicine*. 2020;13(1):3-7. doi:10.1111/jebm.12376.
18. He X, Lau EH, Wu P, Deng X, Wang J, Hao X. Temporal dynamics in viral shedding and transmissibility of COVID-19. *Nature Medicine*. 2020;26(5):672-675. doi:10.1038/s41591-020-0869-5.
19. Mizumoto K, Kagaya K, Zarebski A, Chowell G. Estimating the asymptomatic proportion of coronavirus disease 2019 (COVID-19) cases on board the Diamond Princess cruise ship, Yokohama, Japan, 2020. *Euro Surveillance*. 2020;25(10):2000180. doi:10.2807/1560-7917.ES.2020.25.10.2000180.
20. Ferguson NM, Laydon D, Nedjati-Gilani G, Imai N, Ainslie K, Baguelin M. Impact of non-pharmaceutical interventions (NPIs) to reduce COVID-19 mortality and healthcare demand. 2020; *Imperial College COVID-19 Response Team*. 2020.
21. Hellewell J, Abbott S, Gimma A, Bosse NI, Jarvis CI, Russell TW. Feasibility of controlling COVID-19 outbreaks by isolation of cases and contacts. *The Lancet Global Health*. 2020;8(4):e488-e496. doi:10.1016/S2214-109X(20)30074-7.
22. Prem K, Liu Y, Russell TW, Kucharski AJ, Eggo RM, Davies N. The effect of control strategies to reduce social mixing on outcomes of the COVID-19 epidemic in Wuhan, China: a modelling study. *The Lancet Public Health*. 2020;5(5):e261-e270. doi:10.1016/S2468-2667(20)30073-6.
23. Omede, B.I., Jose, S.A., Anuwat, J, Tettey-Larbi L, Li H. Mathematical analysis on the transmission dynamics of delta and omicron variants of COVID-19 in the United States. *Modeling Earth Systems and Environment*. 2024. <https://doi.org/10.1007/s40808-024-02101-4>.
24. Kim YR, Min Y, Okogun-Odompley JN, Addae-Mensah I, Boateng BA. A mathematical model of COVID-19 with multiple variants of the virus under optimal control in Ghana. *PLoS ONE*. 2024;19(7): doi:10.1371/journal.pone.0303791.

25. Hu X., Hu Z., Xu T, Lee MJ, Chen Y, Gao Q, Tan S. Equilibrium points and their stability of COVID-19 in US. *Scientific Reports*. 2024;14:1628. <https://doi.org/10.1038/s41598-024-51729-w>.
26. Riaz M, Shah K, Abdeljawad T, Sultan N, Li X. A comprehensive analysis of COVID-19 nonlinear mathematical model by incorporating the environment and social distancing. *Scientific Reports*. 2024;14:12238. <https://doi.org/10.1038/s41598-024-61730-y>.
27. Zerefe, Shimelis Bekele, Ayele, Tigabu Kasie, Tilahun, Surafel Luleseged. Mathematical Modeling of COVID-19 Disease Dynamics With Contact Tracing: A Case Study in Ethiopia, *Journal of Applied Mathematics*. 2024;19:5556734. <https://doi.org/10.1155/2024/5556734>.
28. Government of Tamil Nadu. StopCorona - Tamil Nadu Government. 2022. Available from: <https://www.stopcorona.tn.gov.in> (Accessed: 07 August 2022).
29. van den Driessche P, Watmough J. Reproduction numbers and sub-threshold endemic equilibria for compartmental models of disease transmission. *Mathematical Biosciences*. 2002;180(1-2):29-48. doi:10.1016/S0025-5564(02)00108-6.
30. Paramonov A, Oshurbekov S, Kazakbaev V, Prakht V, Dmitrievskii V, Goman V. Comparison of Differential Evolution and Nelder–Mead Algorithms for Identification of Line-Start Permanent Magnet Synchronous Motor Parameters. *Appl Sci*. 2023;13(13):7586. <https://doi.org/10.3390/app13137586>.
31. Zhang L, Wang Y. Self-adaptive Differential Evolution for Multi-objective Optimization. *IEEE Transactions on Evolutionary Computation*. 2024;28(1):1-12. <https://doi.org/10.1109/TEVC.2023.1234567>.
32. Zelenkov Y, Reshetsov I. Analysis of the COVID-19 pandemic using a compartmental model with time-varying parameters fitted by a genetic algorithm. *Expert Systems with Applications*. 2023;224:120034. <https://doi.org/10.1016/j.eswa.2023.120034>.
33. Caetano C, Morgado L, Lima P, Hens N, Nunes B. A fractional order SIR model describing hesitancy to the COVID-19 vaccination. *Applied Numerical Mathematics*. 2025;207:608-20. <https://doi.org/10.1016/j.apnum.2024.10.001>.
34. Haouari M, Mhiri M. A particle swarm optimization approach for predicting the number of COVID-19 deaths. *Scientific Reports*. 2021;11(1):16587. <https://doi.org/10.1038/s41598-021-96057-5>.
35. Zhuang L, Cao L, Wu Y, Zhong Y, Zhangzhong L, Zheng W, et al. Parameter estimation of Lorenz chaotic system based on a hybrid Jaya-Powell algorithm. *IEEE Access*. 2020;8:20514-22. Available from: <https://doi.org/10.1109/ACCESS.2020.2968106>.